Circadian Clock Characteristics Are Altered in Human Thyroid Malignant Nodules

Tiphaine Mannic, Patrick Meyer, Frederic Triponez, Marc Pusztaszeri, Gwendal Le Martelot, Olivia Mariani, Daniel Schmitter, Daniel Sage, Jacques Philippe, and Charna Dibner

Divisions of Endocrinology, Diabetes, Nutrition, and Hypertension (T.M., P.M., J.P., C.D.), Thoracic and Endocrine Surgery (F.T.), and Clinical Pathology (M.P.), University Hospital of Geneva, and Faculty of Medicine (G.M., C.D.), University of Geneva, CH-1211 Geneva, Switzerland; and Biomedical Imaging Group (O.M., D.Sc., D.Sa.), Ecole Polytechnique Fédérale de Lausanne, CH-1015 Lausanne, Switzerland

Context: The circadian clock represents the body's molecular time-keeping system. Recent findings revealed strong changes of clock gene expression in various types of human cancers.

Objective: Due to emerging evidence on the connection between the circadian oscillator, cell cycle, and oncogenic transformation, we aimed to characterize the circadian clockwork in human benign and malignant thyroid nodules.

Design: Clock transcript levels were assessed by quantitative RT-PCR in thyroid tissues. To provide molecular characteristics of human thyroid clockwork, primary thyrocytes established from normal or nodular thyroid tissue biopsies were subjected to in vitro synchronization with subsequent clock gene expression analysis by circadian bioluminescence reporter assay and by quantitative RT-PCR.

Results: The expression levels of the *Bmal1* were up-regulated in tissue samples of follicular thyroid carcinoma (FTC), and in papillary thyroid carcinoma (PTC), as compared with normal thyroid and benign nodules, whereas *Cry2* was down-regulated in FTC and PTC. Human thyrocytes derived from normal thyroid tissue exhibited high-amplitude circadian oscillations of *Bmal1-luciferase* reporter expression and endogenous clock transcripts. Thyrocytes established from FTC and PTC exhibited clock transcript oscillations similar to those of normal thyroid tissue and benign nodules (except for *Per2* altered in PTC), whereas cells derived from poorly differentiated thyroid carcinoma exhibited altered circadian oscillations.

Conclusions: This is the first study demonstrating a molecular makeup of the human thyroid circadian clock. Characterization of the thyroid clock machinery alterations upon thyroid nodule malignant transformation contributes to understanding the connections between circadian clocks and oncogenic transformation. Moreover, it might help in improving the thyroid nodule preoperative diagnostics. **(*J Clin Endocrinol Metab* 98: 4446–4456, 2013)**

Thyroid nodules are frequent, but only 5% of them are malignant (1). Thyroid malignancies of follicular cell origin include well-differentiated papillary (PTCs) and follicular thyroid carcinomas (FTCs), which are the most common. Poorly differentiated (PDTCs) and undifferentiated (anaplastic) thyroid carcinomas (ATCs) (2) are less frequent. Fine-needle aspiration (FNA) biopsy is recommended for the clinical evaluation of thyroid nonsecreting nodules of 1 cm or greater. FNA is currently the most accurate and safe tool in the management and classification of patients with thyroid nodules. Thyroid FNA represents a test of choice for preoperative diagnostic in PTC

ISSN Print 0021-972X ISSN Online 1945-7197
Printed in U.S.A.
Copyright © 2013 by The Endocrine Society
Received June 19, 2013. Accepted August 16, 2013.
First Published Online August 26, 2013

Abbreviations: *BMAL1*, brain and muscle aryl hydrocarbon receptor nuclear translocator-like protein 1; *CRY*, cryptochrome; *Dbp*, D-site albumin promoter binding protein; FNA, fine-needle aspiration; FTC, follicular thyroid carcinoma; PDTC, poorly differentiated thyroid carcinoma; PDTC-PTC, poorly differentiated thyroid carcinoma developed on PTC; *Per*, period; PTC, papillary thyroid carcinoma; qPCR, quantitative PCR; Timp1, tissue inhibitor of metalloproteinase 1.

The Endocrine Society. Downloaded from press.endocrine.org by [${individualUser.displayName}] on 04 May 2015. at 05:40 For personal use only. No other uses without permission. . All rights reserved.

cases, allowing reliable recognition of this malignancy type. In cases of FTC, however, FNA does not allow clear discrimination between benign follicular lesions (nodular hyperplasia, adenomatous goiter, and follicular adenoma) and a malignant follicular lesion (FTC) and thus represents only a screening test. Therefore, surgery is required for all lesions diagnosed as suspicious for a follicular neoplasm and for some of the lesions of undetermined significance (3). Postoperatively, 70%–90% of these cases are found to be benign, revealing a significant rate of unnecessary surgery, complications, and morbidity (4). Multiple ultrasonography and immunohistochemical or genetic features have been associated with malignancy, but none of them is by itself sufficiently accurate to distinguish follicular adenoma from carcinoma with high probability (5). The search for preoperative markers for thyroid malignancies stays therefore of utmost clinical importance.

Circadian oscillation of biological processes has been described in virtually all light-sensitive organisms. It reflects the existence of intrinsic clocks with near 24-hour oscillation periods. The mammalian clock has a hierarchical structure, in which a master pacemaker residing in the brain's suprachiasmatic nuclei must establish phase coherence in the body by synchronizing billions of individual cellular clocks every day (6). Central and peripheral clocks have a similar molecular makeup. Moreover, this rhythm generating circuitry is functional in most cell types (7). In addition to an intrinsic circadian oscillator, another fundamental attribute of a cell is its ability to divide and multiply. Whereas the circadian clock is the body's molecular time-keeping system, the cell division clock executes a precise temporal control mechanism with multiple checkpoints for proper cell division. Recent findings revealed that circadian and cell cycle clocks might be linked (7–9). Furthermore, clock genes have been linked to the cell cycle, DNA damage, apoptosis control, and carcinogenesis (10–12). Perturbation of circadian rhythms both in humans (shift workers) and animals has been associated with malignant transformations (13). Taken together, these data suggest a strong link between the circadian clock and the cell cycle.

Turning to the thyroid gland regulating hormones, both TRH and TSH exhibit pronounced circadian oscillations in the blood with a peak between 2:00 AM and 4:00 AM in healthy subjects. Moreover, low-amplitude circadian variations were reported for the thyroid hormones [total T_3 and T_4 (14)], suggesting circadian function for the thyroid gland. We therefore aimed at characterizing the clock machinery in human healthy thyroid tissue and in benign and malignant thyroid nodules.

Materials and Methods

Study participants and thyroid tissue sampling

Fresh thyroid tissue samples (1 cm^3) were obtained from patients undergoing thyroidectomy for thyroid cancer or suspicious nodule, with the written informed consent. Donor characteristics are summarized in Table 1. The subjects were not kept on a constant routine prior to the surgery. The biopsy material was collected in a daytime-dependent manner, with all the surgeries performed in the time window between 8:00 AM and 2:00 PM. The study protocol was approved by the local Ethics Committee (CER 11–014). Malignant tumors were classified by histopathological analysis according to the World Health Organization Histological Classification of Thyroid Tumors (15) and staged according to the *American Joint Committee on Cancer Cancer Staging Manual*, seventh edition. One part of the obtained thyroid tissue was deep frozen and kept for tissue transcript analysis; the other part was immediately processed to establish primary culture.

Human primary thyroid cell culture

Fresh tissue biopsies were subjected to type II collagenase (Life Technologies) digestion for 1 hour. Cells were grown in DMEM supplemented with 10% fetal bovine serum and 1% penicillin/streptomycin. Primary thyrocytes were used for the experiments after reaching confluence, typically after 7 days of culture.

In vitro cell synchronization

To synchronize thyrocytes, dexamethasone was added to the culture medium at a final concentration of 100 nM. After 30 minutes of incubation at 37°C in a cell culture incubator, dexamethasone was washed away and replaced with normal medium, as described (16). Cells were harvested every 6 hours during 36 hours, deep frozen, and kept at −80°C.

RNA extraction and quantitative RT-PCR (qPCR) analysis

Total RNA from frozen thyroid biopsies or thyrocytes was prepared using RNA spin II kit (Macherey-Nagel). Tissue biopsies were first homogenized using a Polytron homogenizer. Half a microgram of RNA was reverse transcribed using Superscript III reverse transcriptase (Invitrogen) and random hexamers, PCR amplified, and quantified as previously described (17). Mean values for each experiment were calculated from technical triplicates of PCR assays for each sample and normalized to the mean of those obtained for *GAPDH* and *9S* transcripts served as internal controls. The primers used for this study are listed in Supplemental Table 1, published on The Endocrine Society's Journals Online web site at http://endo.endojournals.org.

Lentivectors and lentiviral production

Bmal1-luciferase (Bmal1-luc) (18) lentiviral particles were produced as previously described (17), 100-fold concentrated, and used for the transduction of thyrocytes at a multiplicity of infection of 5.

The Endocrine Society. Downloaded from press.endocrine.org by [${individualUser.displayName}] on 04 May 2015. at 05:40 For personal use only. No other uses without permission. . All rights reserved.

Table 1. Patient Characteristics and Diagnosis

Donor	Sex	Age, y	Time of Surgery	Cytological Diagnostics
Benign thyroid samples				
H11014994[a,b]	F	48	10 h 30 min	Adenoma
H11011188[a,b]	F	80	9 h	Hyperplasia
H11001549	F	70	9 h 30 min	Adenoma
H12000211[b,c]	F	39	10 h 30 min	Hyperplasia
H12011256[a,b,c]	F	58	9 h 30 min	Hyperplasia
H12012922[b,c]	F	40	9 h	Multinodular goiter
H12013740	F	57	10 h 30 min	Multinodular goiter
H12013289	M	49	10 h 30 min	Adenoma
H12013281	F	52	8 h 20 min	Adenoma
H12010459	F	46	8 h 25 min	Adenoma
H12014865	F	53	9 h	Multinodular goiter
H12012567	F	39	10 h	Multinodular goiter
Total benign (n = 12 patients)	M, n = 1; F, n = 11	52.5 ± 12.4	9 h 40 min ± 0 h 40 min	
Malignant thyroid samples				
FTC				
H12009322[c]	F	38	9 h 30 min	FTC pT3
H13000118[c]	F	48	13 h	FTC pT2
H13001153	F	70	11 h 05 min	FTC pT3N1b
H13000118	F	49	12 h 25 min	FTC pT2
H09012394	M	32	10 h	FTC pT3Nx
H08014112	F	36	12 h 30 min	FTC pT2Nx
H07008276	F	36	ND	FTC pT2Nx
H12014817	F	48	10 h	FTC pT2
Total FTC (n = 8 patients)	M, n = 1; F, n = 7	44.6 ± 12.2	11 h 15 min ± 1 h 30 min	
PTC				
H12007145[c]	M	29	9 h 30 min	PTC pT3pN0
H12014994[c]	F	38	11 h	FV PTC
H13001254	M	64	13 h	PTC pT3 pN0
H12013965	F	51	12 h 50 min	PTC pT3 pN1a
H12012290	M	26	8 h 30 min	PTC pT2 pN1a (6/11)
H12012070	M	56	13 h 30 min	PTC pT1b pN0
H12011540	F	73	14 h	PTC pT3 pN1a
H12010429	F	57	13 h 10 min	PTC pT3 Nx
H12003781	F	55	12 h 30 min	PTC pT3 pN0
H11009795	F	29	11 h	PTC pT2 pN0
H10003462	F	65	8 h 30 min	PTC pT3Nx
H10001114	F	50	8 h 30 min	PTC pT3 pN1a
H12006309	F	38	12 h 30 min	PTC pT3 pN1a
H12007402[c]	F	40	13 h	PTC pT3 pN1b
Total PTC (n = 14 patients)	M, n = 4; F, n = 10	50.3 ± 14.5	11 h 45 min ± 2 h	
PDTC				
H12010398[c]	M	47	9 h	PTC/PDTC pT3
PDTC-PTC				
H13000386[a,c]	F	20	13 h	PTC/PDTC pT2
Total malignant (n = 24 patients)	M, n = 6; F, n = 18	45.6 ± 14.2	11 h 15 min ± 1 h 40 min	
Total (n = 36 patients)	M, n = 7; F, n = 29	49 ± 14.5	11 h ± 1 h 40 min	

Abbreviation: ND, surgery timing was not defined. TN(M) classifications included the following: primary tumor (T) including T2, with a tumor size greater than 2 cm but 4 cm or less, limited to the thyroid; and T3, with a tumor size greater than 4 cm, limited to the thyroid or any tumor with minimal extrathyroidal extension (eg, extension to sternothyroid muscle or perithyroid soft tissues); and regional lymph nodes (N) including NX, with regional nodes that cannot be assessed; N0, with no regional lymph node metastasis; N1, with regional lymph node metastasis; N1a, with metastases to level VI (pretracheal, paratracheal, and prelaryngeal/delphian lymph nodes); and N1b, with metastases to unilateral, bilateral, or contralateral cervical (levels I, II, III, IV, or V) or retropharyngeal or superior mediastinal lymph nodes (level VII).

[a] Tissue samples used for circadian bioluminescence assay.

[b] Healthy thyroid tissue samples adjacent to the nodule were used as healthy control.

[c] Tissue samples used for primary thyrocyte culture.

The Endocrine Society. Downloaded from press.endocrine.org by [${individualUser.displayName}] on 04 May 2015. at 05:40 For personal use only. No other uses without permission. . All rights reserved.

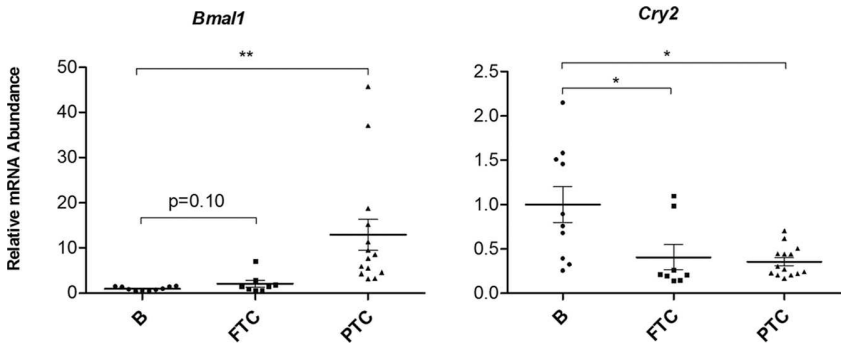

Figure 1. Expression of core-clock genes in tissue biopsies of benign thyroid nodules, FTCs and PTCs. qPCR for *Bmal1* and *Cry2* was performed on cDNAs obtained from tissue samples from nodules with benign (n = 10), FTC (n = 8), and PTC (n = 14) postoperatory diagnosis. The relative mRNA expression of each transcript was normalized to the average of *Gapdh* and *9S* and then reported to the mean value of the respective transcript levels in nodular benign tissues. Results were expressed as mean ± SEM. A Mann-Whitney *U* test was applied to assess the significance in the transcript expression level differences between FTCs or PTCs as compared with benign nodules. *, $P < .05$; **, $P < .01$; ***, $P < .001$.

Bioluminescence monitoring

Bioluminescence patterns were monitored from dexamethasone synchronized human thyrocytes 4 days after *Bmal1-luc* lentiviral transduction, as previously described (16, 17). Briefly, synchronized cells were transferred to Actimetrics LumiCycle placed in a 37°C light-tight incubator, and bioluminescence from each dish was continuously monitored using a Hamamatsu photomultiplier tube detector assembly. An Actimetrics LumiCycle analysis program was used to assess the rhythm parameters.

Cosinor analysis

To quantify circadian oscillatory gene expression profiles, we have developed new software CosinorJ, based on a cycling function model representing the extension of the standard Cosinor method (19):

$$(A + Bt)\cos\left(\frac{2\pi}{T}(t-\omega)\right) + C$$

where T is the period, A+Bt is the range of oscillations, C is the mesor, and ω is the acrophase (see Supplemental Methods for details). It is freely available (http://bigwww.epfl.ch/algorithms/cosinorj/).

Statistics

The results are expressed as the means ± SEM unless stated otherwise. A Mann-Whitney *U* test was applied to compare transcript expression levels between the different tissue types.

Results

Bmal1 transcript is up-regulated, whereas *Cry2* is down-regulated in FTC and PTC nodule tissues

In an attempt to assess core-clock transcript levels in benign and malignant thyroid tissues, biopsies from human normal thyroid tissue, benign follicular nodules, FTCs, or PTCs were obtained after thyroidectomy (see Table 1 for patient characteristics). The qPCR analysis of core-clock transcripts was performed in healthy thyroid tissue (n = 4 subjects), benign thyroid nodules (n = 10 subjects), FTC (n = 8 subjects) and PTC nodules (n = 14 subjects). No difference was observed between healthy tissue and benign nodules for all of the analyzed transcript expression levels (data not shown). By contrast, *Bmal1* expression was 13-fold up-regulated, whereas *Cry2* (cryptochrome) expression was about 2-fold down-regulated in PTCs compared with benign nodules (Figure 1 and Supplemental Table 2). In FTC, *Bmal1* exhibited 2-fold up-regulated levels, whereas *Cry2* was 2-fold down-regulated (Figure 1 and Supplemental Table 2). Transcript levels of *Cry1*, *Per1*, *Per2*, *Per3*, *Reverbα*, and *Dbp* (D-site albumin promoter binding protein) in PTCs and FTCs were either indistinguishable or not significantly changed, as compared with benign counterparts (Supplemental Table 2). In addition to the core-clock transcript changes, we found up-regulated levels of *Timp1* (tissue inhibitor of metalloproteinase 1) and down-regulated levels of *Gadd153* transcripts in PTCs (Supplemental Figure 1A, left panel, and 1B). This finding is in a good agreement with previous publications (20, 21). Of note, significant correlation was observed between *Timp1* and *Bmal1* transcript levels obtained in PTCs (Supplemental Figure 1A, right panel), further validating our conclusion regarding *Bmal1* up-regulation.

Self-sustained circadian oscillators are operative in human primary thyrocytes

Prompted by marked differences in core-clock transcript levels between benign and malignant thyroid tissues, we next aimed at characterizing the human thyroid clock molecular makeup. Given obvious obstacles for studying peripheral clocks in human beings, we used cultured human primary thyrocytes synchronized in vitro. Cells were established from fresh normal thyroid tissue obtained after thyroidectomy (Table 1, samples labeled with c). To confirm thyrocyte cell identity, thyroglobulin expression was assessed by indirect immunofluorescence. Thyroglobulin was detected in 75.3% of cells (1232 positive of total 1634 cells) after 7 days in culture (Supplemental Figure 2).

To assess the endogenous core-clock transcript expression profiles around the clock, confluent primary thyrocytes were synchronized by a dexamethasone pulse because dexamethasone has been previously demonstrated to synchronize efficiently circadian oscillators in various

The Endocrine Society. Downloaded from press.endocrine.org by [${individualUser.displayName}] on 04 May 2015. at 05:40 For personal use only. No other uses without permission. . All rights reserved.

cellular systems (17, 22). mRNA accumulation patterns from synchronized thyrocytes were monitored every 6 hours during 36 hours by quantitative RT-PCR, using amplicons for *Bmal1*, *Cry1*, *Cry2*, *Per1*, *Per2*, *Per3*, *Reverbα*, and *Dbp*. The values were normalized to the average obtained for *Gapdh* and *9S* transcripts, which accumulated to similar levels throughout the day. Endogenous *Bmal1* transcript abundance exhibited high-amplitude circadian oscillations, in phase with *Cry1*, and antiphasic to those of *Reverbα*, *Per1–3*, and *Dbp* transcripts (Figure 2), in good agreement with previous studies on human skin dermal fibroblasts (23) and human pancreatic islets (17). *Cry2* mRNA exhibited weak oscillatory profile, in phase with *Reverbα*, as expected from previous studies (17). For the quantification of these data sets, we used CosinorJ software, representing the optimization of the existing Cosinor method (19) to the cases with few circadian time points over short time (see *Materials and Methods*). CosinorJ analysis revealed that *Bmal1*, *Per1–3*, and *Reverbα* exhibited clear circadian oscillations with a period length of 28.06 ± 1.44 hours (mean ± SEM), mesor comprised in a 0.63–1.00 interval, and acrophase of 17.31 hours for *Bmal1*, and 31.01–34.78 hours for *Reverbα* and *Per1–3* (Table 2). On the other hand, *Cry1*, *Cry2*, and *Dbp* were considered as nonoscillating according to the fit (Supplemental Figure 3). Taken together, our experiments reveal the presence of cell-autonomous self-sustained circadian oscillators in in vitro synchronized human primary thyrocytes, with the characteristics comparable with other human peripheral tissues.

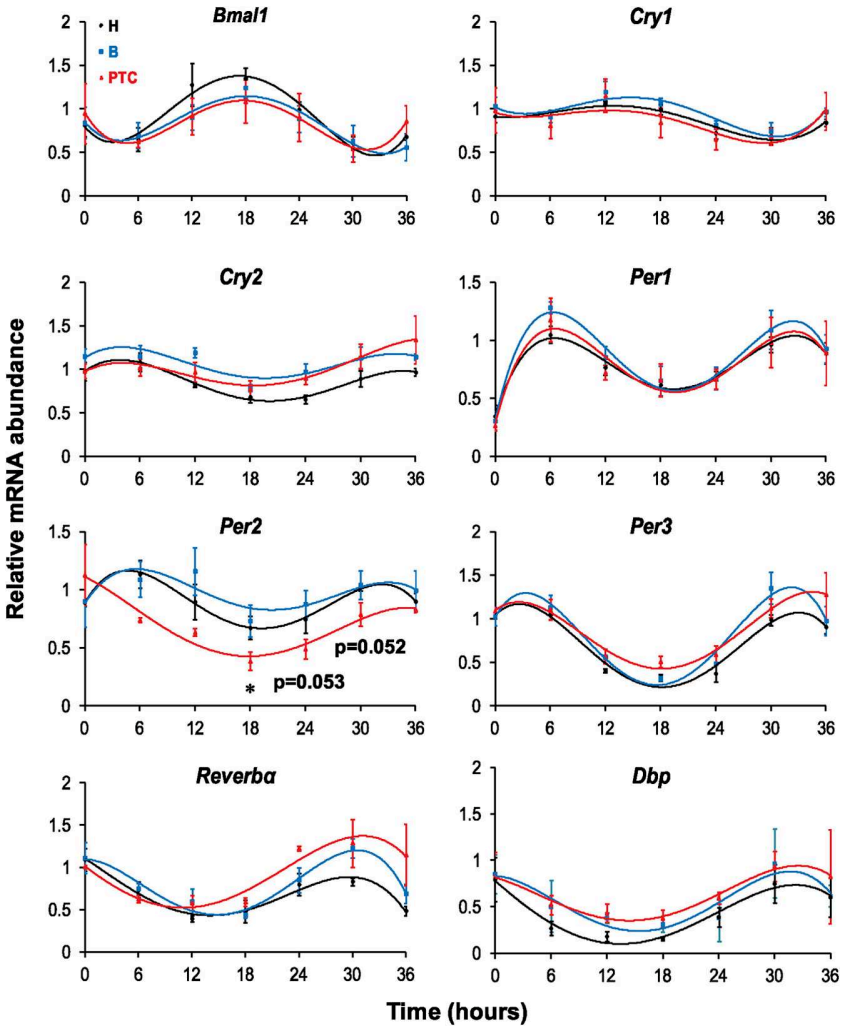

Figure 2. Cell-autonomous, high-amplitude circadian oscillations of clock genes in primary human thyrocytes derived from healthy tissue, benign nodule, and PTC. Oscillation of endogenous clock transcripts was monitored in human primary thyrocytes synchronized with dexamethasone pulse (100 nM, 30 min pulse). qPCR was performed on cDNAs obtained from thyrocyte samples for core-clock (*Bmal1*, *Reverbα*, *Per1–3*, and *Cry1–2*) and clock-controlled (*Dbp*) transcripts and normalized to the average of *Gapdh* and *9S* housekeeping gene expression for each transcript. Profiles are representative of three experiments (mean ± SEM), each using cells from one donor for every cell type. H, healthy thyrocytes (black lines); B, benign nodule derived thyrocytes (blue lines); PTC, PTC-derived thyrocytes (red lines).

The Endocrine Society. Downloaded from press.endocrine.org by [${individualUser.displayName}] on 04 May 2015. at 05:40 For personal use only. No other uses without permission. . All rights reserved.

Table 2. CosinorJ Analysis

	Bmal1				
	H	**B**	**PTC**	**PDTC-PTC**	**PDTC**
Amplitude	0.59	0.41	0.37	0.02[a]	0.38
Mesor	1.00	0.99	0.98	0.92	0.88
Acrophase, h	17.312	17.67	18.50	14.28[a]	9.98[a]
	Per1				
	H	**B**	**PTC**	**PDTC-PTC**	**PDTC**
Amplitude	0.47	0.49	0.35	Noncircadian	Noncircadian
Mesor	0.69	0.66	0.77		
Acrophase, h	31.01	31.91	27.93		
	Per2				
	H	**B**	**PTC**	**PDTC-PTC**	**PDTC**
Amplitude	0.34	0.39	Noncircadian	0.40	0.43
Mesor	0.85	0.93		0.77	0.71
Acrophase, h	33.31	34.34		39.79[a]	25.549[a]
	Per3				
	H	**B**	**PTC**	**PDTC-PTC**	**PDTC**
Amplitude	0.46	0.39	0.35	0.16[a]	0.49
Mesor	0.72	0.71	0.84	0.25[a]	0.64
Acrophase, h	34.78	33.1	35.96	31.67[a]	27.85[a]
	Reverbα				
	H	**B**	**PTC**	**PDTC-PTC**	**PDTC**
Amplitude	0.42	0.46	0.36	0.10[a]	0.69
Mesor	0.63	0.77	0.78	0.54	0.84
Acrophase, h	34.04	30.54	29.55	31	20.7[a]

Data were obtained with qPCR analysis and presented in Figures 2 and 3 and were fit by CosinorJ, and the oscillation parameters (amplitude, mesor, and acrophase) were calculated by this software. The profiles with the periods out of circadian range (20–35 h) or ablated circadian amplitude were defined as noncircadian by CosinorJ. H, Healthy thyrocytes; B, benign nodule derived thyrocytes.

[a] The values were significantly altered in comparison with normal and benign nodular thyrocytes.

Circadian characteristics of the human nodular primary thyrocytes established from benign and malignant thyroid nodules

To study possible clock alterations in thyroid malignancies, we assessed oscillatory profiles of human primary thyrocytes derived from nodules with benign or malignant histopathological diagnosis such as FTC (Supplemental Figure 4), PTC (Figure 2), and PDTC (Figure 3; see Table 1 for diagnosis details). Primary thyrocytes derived from nodular tissues were established and grown as described above for normal thyrocytes. Thyroglobulin staining was performed in all cell types after 7 days in culture and was positive in 77.3% of cells for benign nodule-derived thyrocytes (729 positive of 942 cells), 72% for FTC derived thyrocytes (532 of 738 cells), 71.9% for PTC thyrocytes (295 of 410 cells), and 93% for PDTC thyrocytes (243 of 261 cells; Supplemental Figure 2). Therefore, our analyses report circadian properties of 71.9%–93% of human primary thyrocytes with the residual amount of contaminant cells, mostly fibroblasts.

Human primary thyrocytes established from benign nodules exhibited circadian oscillations with similar characteristics to those of normal thyrocytes (Figure 2, compare blue and black lines). CosinorJ analysis (performed in all cases as depicted in Supplemental Figure 3) revealed that, similarly to normal primary thyrocytes, primary cells established from benign nodules exhibited an oscillation period of 27.99 ± 1.93 hours. *Bmal1*, *Per1–3*, and *Reverbα* transcripts exhibited pronounced circadian oscillatory patterns with mesor, amplitude, and acrophase close to those of normal thyrocytes (Table 2), whereas *Cry1–2* and *Dbp* profiles did not fit CosinorJ criteria for circadian pattern.

Analysis of endogenous clock transcripts in primary thyrocytes established from FTCs revealed no significant differences for all of the analyzed clock transcripts when

The Endocrine Society. Downloaded from press.endocrine.org by [${individualUser.displayName}] on 04 May 2015. at 05:40 For personal use only. No other uses without permission. . All rights reserved.

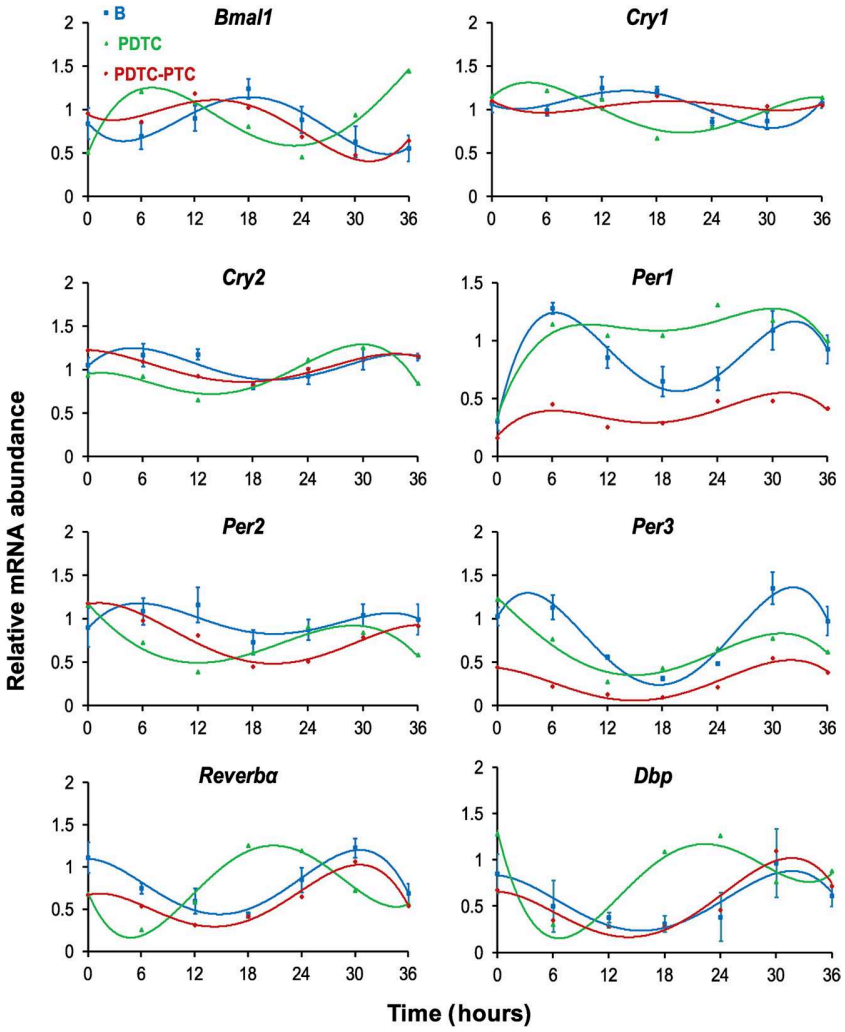

Figure 3. Oscillation profiles of clock genes are altered in primary thyrocytes derived from PDTCs and PDTC-PTCs (single case studies). qPCR analysis was performed in dexamethasone-synchronized thyrocytes in the samples collected around the clock for *Bmal1*, *Reverbα*, *Per1–3*, *Cry1–2*, and *Dbp* transcripts and normalized to the average of *Gapdh* and *9S* housekeeping gene expression for each transcript. Profiles for benign thyroid nodule (blue lines) correspond to those presented in Figure 2 as mean ± SEM of three experiments. Profiles for PDTC- (green lines) and PDTC-PTC-derived thyrocytes (red lines) represent a single donor each.

compared with the thyrocytes derived from benign nodules (Supplemental Figure 4) or with normal thyrocytes (not shown). Period length, amplitude, and acrophase were similar between FTC and thyrocytes established from benign nodules for all of the transcripts, with *Bmal1*, *Per1–3*, and *Reverbα* showing pronounced circadian oscillations. Oscillatory profiles of *Bmal1*, *Cry1*, *Cry2*, *Per1*, and *Per3* transcripts assessed in synchronized PTCs derived thyrocytes were similar to those of benign nodular and normal thyrocytes (Figure 2). CosinorJ analysis revealed, however, a reduced circadian amplitude for *Per2* in PTC and no fit to the circadian pattern for this transcript (Table 2). Thus, clock transcripts in PTC thyrocytes keep their oscillatory properties, except for *Per2* exhibiting altered circadian profile (Figure 2 and Table 2). Remarkably, analysis of the primary thyrocytes established from a single case of PDTC revealed altered oscillatory profiles for all of the analyzed transcripts (Figure 3). Namely, *Per1* transcripts exhibited ablated circadian amplitude, whereas *Bmal1*, *Per2–3*, and *Reverba* transcripts were strongly phase shifted in comparison with the thyrocytes derived from benign nodules (marked differences in acrophase values; see Table 2). Furthermore, an additional single case analysis of primary thyrocytes established from a mixed PDTC-PTC showed flatter amplitude and phase-shifts for all of the transcripts (Figure 3 and Table 2). Taken together, these experiments reveal that although thyrocytes from benign nodules perfectly keep their circadian properties, alterations in the clock gene profiles are observed in in vitro-synchronized thyrocytes established from PTCs and PDTCs.

The rhythm alterations we observed in PTC- and PDTC-derived thyrocytes might be attributed to the circadian phase alteration solely or to the changes in the circadian period length. To assess the human thyrocyte circadian properties beyond the first cycle kinetics, we turned to more sensitive methodology based on long-term continuous circadian bioluminescence oscillation recording with high temporal resolution. Indeed, human fibroblasts and human islet cells expressing firefly luciferase from circadian promoters were previously shown to exhibit robust circadian bioluminescence rhythms after in vitro synchronization (17, 23). We thus monitored circadian bioluminescence of human primary thyrocytes transduced with *Bmal1-luciferase* lentivectors, synchronized by dexamethasone pulse. Oscillation patterns were assessed in healthy, nodular benign and PDTC-PTC-derived thyrocytes (Figure 4). High-amplitude circadian bioluminescence cycles with the period length of 27.45 ± 0.81 hours and 27.90 ± 0.76 hours (n = 3 subjects, labeled with a in Table 1) were detected in primary thyrocytes derived from normal tissues and benign nodules for at least 3 consecutive days, in a good agreement with the endogenous transcript analysis. Of note, PDTC-PTC thyrocytes exhibited remarkably shifted or even antiphasic profiles of *Bmal1-luc* reporter oscillatory expression over the first cycle only and getting in phase with healthy and benign nodular counterparts

The Endocrine Society. Downloaded from press.endocrine.org by [${individualUser.displayName}] on 04 May 2015. at 05:40 For personal use only. No other uses without permission. . All rights reserved.

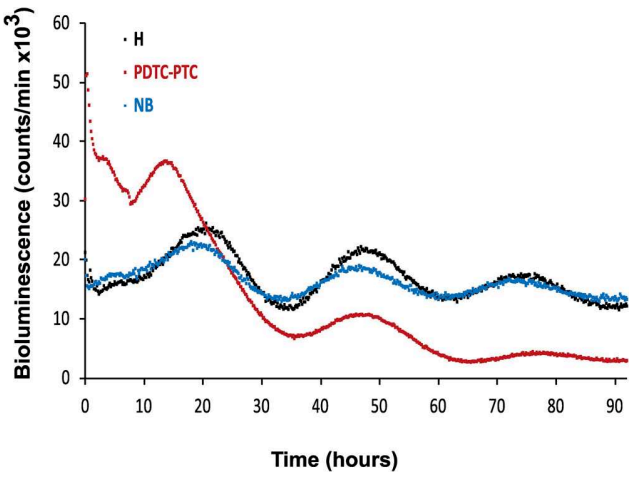

Figure 4. Circadian oscillations of *Bmal1-luciferase* reporter in human primary thyrocytes. *Bmal1-luciferase* oscillations were recorded in in vitro-synchronized human primary thyrocytes derived from healthy tissue (H), benign thyroid nodule (NB), or PDTC-PTC: black, blue, and red lines, respectively). Cells were transduced with *Bmal1-luciferase* lentivectors, synchronized 4 days later with a dexamethasone pulse, and *Bmal1-luciferase* bioluminescence profiles were recorded for two parallel dishes for each donor (n = 3 donors for thyrocytes derived from healthy tissue and benign nodules; n = 1 donor for PDTC-PTC). The curves represent an average of all the performed recordings for each cellular type.

over the following second and third circadian cycles. This experimental approach outcome provides a clear-cut confirmation of the presence of functional circadian oscillators in human primary thyrocytes originated from healthy and benign nodular tissues. Moreover, it suggests that the phase shifts observed in PDTC-PTC-derived cells as compared with the benign counterparts are attributed to the first cycle kinetics change and do not imply the circadian period length alterations.

Discussion

Molecular makeup of human thyroid clock

Our study provides for the first time an evidence for cell-autonomous, high-amplitude circadian oscillators functional in cultured human primary thyrocytes established from healthy thyroid tissue. Thyrocyte oscillations were assessed by two approaches. Continuous recording of circadian bioluminescence produced by a stably integrated *Bmal1-luciferase* reporter gene represents a powerful and rather unique tool for circadian oscillator studies in living human primary explants or cells for several consecutive days with high temporal resolution. Dexamethasone synchronized human thyrocytes transduced with *Bmal1-luciferase* lentivectors exhibited pronounced circadian oscillations for at least 90 hours after synchronization (Figure 4). In line with the outcome of reporter experiments, endogenous clock gene expression measurements by qPCR suggested that the core-clock transcripts exhibit circadian oscillatory patterns in synchronized thyrocytes (Figure 2). Both approaches suggested circadian period of about 27 hours for this type of cells. Previously circadian time keepers were characterized in human primary skin fibroblasts and in human pancreatic islets synchronized in culture (17, 23). In terms of the phase of core-clock transcripts our work is in a good agreement with previous studies. Human thyrocytes exhibit longer oscillation period if compared with skin fibroblasts (24.5 h) or human pancreatic islets [23.6 h (17, 23)]. Of note, circadian oscillation period length varies significantly among different mouse organ explants cultured in vitro (24), probably reflecting the differences in the general transcriptional rates and cell size among these organs, if comparing liver and lung, for example (16, 25).

Thyrocyte oscillator properties change upon thyroid nodule malignant transformation

A central question addressed in this study was whether circadian clockwork is altered upon thyroid malignancies. We found that transition of normal thyroid tissue to the benign nodule does not alter circadian oscillator function. This held true for both circadian bioluminescence analysis of the cells expressing circadian reporter and for the endogenous transcript analysis (Figures 4 and 2, respectively). However, around-the-clock analysis of cells established from PTCs and PDTCs suggested that malignant transformation of human primary thyrocytes might change their circadian oscillator properties (Figures 2–4 and Table 2). Although in general the oscillators are functional in FTC- and PTC-derived thyrocytes, *Per2* transcript oscillatory profile was altered in PTCs (Supplemental Figure 4, Figure 2, and Table 2). This tendency becomes more obvious when looking at *Per1–3* transcript profiles in PDTC samples (Figure 3 and Table 2), in which the amplitude is flattened with complete loss of the oscillatory pattern in *Per1*. Most importantly, we observed dramatic changes in all circadian transcript phase in PDTC, with some of the transcripts being antiphasic to benign counterparts (Figure 3 and Table 2).

Observing circadian profiles in PDTC-PTC-derived thyrocytes over several consecutive days with high temporal resolution (Figure 4), we conclude that these changes are limited to the phase shift of the first circadian peak, in an agreement with our qPCR measurements (Figure 3), whereas later on PDTC cell profile aligns with healthy and benign counterparts (Figure 4). This change attributed to the kinetics of the first circadian cycle might suggest the alteration of clock immediate resetting response in PDTC-derived cells. To get further insights to the nature of these alterations, single-cell analysis by bioluminescence time-lapse microscopy of benign vs PDTC thyrocytes will be

The Endocrine Society. Downloaded from press.endocrine.org by [${individualUser.displayName}] on 04 May 2015. at 05:40 For personal use only. No other uses without permission. . All rights reserved.

required. It is not excluded that glucocorticoid hormones, commonly used by us and others for in vitro cell synchronization and playing an important role for peripheral clock synchronization in vivo (6, 26), might also play a role in thyroid clock regulation in vivo. Another plausible candidate for the thyroid clock synchronization stimulus would be TSH, exhibiting strongly oscillating profile in the blood (14, 27). Of note, the level of TSH receptor in thyrocytes was found to be decreased in PTC (28). It will be interesting to address in the future whether indeed TSH might play a role in thyroid cell synchronization and whether the down-regulation of the TSH receptor in PTC might impact on oscillator synchronization properties in these cells.

Two major factors limit the interpretation of our experiments: the low number of available fresh postoperative material of the malignant nodules and the low number of the primary cells we could establish from each biopsy. Therefore, although the reproducibility among the around-the-clock experiments was high, these experiments must be taken with caution due to the low number of the analyzed cell lines. The number of cells derived per biopsy allowed performing around-the-clock analysis with 6 hours of resolution over 36 hours, seven circadian time points in total. To make the analysis of these data set more robust, we developed an adaption of the existing software packages already available for this type of data set analysis (29–31). Our new software, CosinorJ, represents an efficient, fast, user-friendly tool for oscillating data set analysis, freely available for the research community.

Bmal1 and *Cry2*: potential candidates for FTC and PTC preoperative diagnostic markers

Importantly, our study reveals strong alterations of core-clock transcripts *Bmal1* and *Cry2* in FTC and PTC, when compared with benign nodules and healthy tissue samples taken at a similar time window of the day (Figure 1). We demonstrate for the first time that core-clock gene expression levels are altered in thyroid malignancies, namely the up-regulation of *Bmal1* and down-regulation of *Cry2* in FTCs and PTCs. Moreover, *Bmal1* transcript levels were positively correlated with those of *Timp1,* also up-regulated in the same PTC samples [Supplemental Figure 1A (20)]. This correlation further underscores a potential link between *Bmal1* expression level and possibly function and thyroid nodule tumor progression. Of note, we observe more pronounced differences for core-clock transcript levels in biopsy tissue analysis when compared with our experiments done in in vitro synchronized PTC-derived thyrocytes. This discrepancy might be associated with the drastic changes in the cellular environment in in vitro culture situation, associated with the absence of neural and hormonal regulation, disruption of 3-dimensional tissue structure and alterations in cell-cell communication, changes in epigenetic regulation, and influence of additional factors. Those limitations must be taken into account when drawing conclusions from clock in vitro studies in synchronized cultured cells, although this approach stays rather unique when applied to human circadian clock studies.

There is accumulating evidence on the important role of core-clock components for cell cycle progression and timing of cell division. The circadian oscillator gates cytokinesis to defined time windows in in vitro-cultured fibroblasts (7) and regulates key components of the cell cycle *wee1, cyclinB1*, and *cdc2* in mouse liver cells in vivo (9). Of note, *Per2* plays a key role as a tumor suppressor by regulating DNA damage responsive pathways (10). Moreover, altered expression levels of several clock genes have been described in various types of malignancies: *Per1–3* were down-regulated in breast cancer (32); *Per1–2*, *Clock*, and *Cry1* were decreased in skin melanoma (33); most of the core-clock transcripts were down-regulated in head and neck squamous cell carcinoma (34), in pancreatic ductal adenocarcinoma (35), and in chronic myeloid leukemia (36).

In line with these studies, our experiments demonstrate down-regulation of *Cry2* levels upon thyroid malignancies. *Bmal1* levels were strongly up-regulated in PTCs and moderately up-regulated in FTCs, suggesting that the up-regulation of this core-clock transcript might be associated with the pathological conditions as well as its down-regulation, demonstrated in the human studies cited above for its association with malignancies, or in a *Bmal1* knockout study revealing an association with reduced life span and premature aging in mice (37). Taken together, these findings further underscore the link between circadian oscillatory function and cellular malignant transformation. Given that preoperative diagnostics of malignant thyroid nodules is still far from providing reliable responses in numerous cases of suspicious or indeterminate nodules (5), it would be important to launch a prospective study for *Bmal1* and *Cry2* transcripts in thyroid nodules to explore the potential use of these transcript changes for improving FTC and PTC preoperative diagnostics.

In conclusion, we present the first detailed characterization of the human thyroid circadian clockwork and its changes upon malignant transformation. These new insights into the core-clock changes upon thyroid malignancies should contribute to the unresolved issue of the malignant nodule preoperative diagnosis. Exploring human thyroid clock function and its potential role in thyroid nodule malignant transformation represents an important

The Endocrine Society. Downloaded from press.endocrine.org by [${individualUser.displayName}] on 04 May 2015. at 05:40 For personal use only. No other uses without permission. . All rights reserved.

step forward in our understanding of the molecular link between clock function, thyroid tissue physiology and pathophysiology of malignant thyroid nodules.

Acknowledgments

We are grateful to Francis Levi for invaluable discussions and critical reading of the manuscript, Camille Saini for constructive comments on this work, Laurent Perrin and Anne-Marie Makhlouf for assistance with the experiments, Jolanta Gourmaud and Philippe Botteron for thyroid biopsy samples, and Christelle Barraclough and Mylene Docquier for help in performing the qPCR experiments.

Address all correspondence and requests for reprints to: Dr Charna Dibner, Department of Endocrinology, Diabetes, Nutrition, and Hypertension, University Hospital of Geneva, 4 Rue Gabrielle-Perret-Gentil, CH-1211 Geneva 14, Switzerland. E-mail: charna.dibner@hcuge.ch.

This work was supported by the Fondation pour la Recherche sur le Cancer et la Biologie (to PM and CD), the Fonds de Recherche du Département des Spécialités de Médecine (to T.M., P.M., and C.D.), and the Fondation Endocrinologie (to C.D.).

Disclosure Summary: The authors declare no conflict of interest.

References

1. **Gharib H.** Fine-needle aspiration biopsy of thyroid nodules: advantages, limitations, and effect. *Mayo Clin Proc*. 1994;69:44–49.
2. **Ibrahimpasic T, Ghossein R, Carlson DL, et al.** Poorly differentiated thyroid carcinoma presenting with gross extrathyroidal extension: 1986–2009 Memorial Sloan-Kettering cancer center experience. *Thyroid*. 2013;23(8):997–1002.
3. **Cibas ES, Ali SZ.** The Bethesda System for Reporting Thyroid Cytopathology. *Thyroid*. 2009;19:1159–1165.
4. **Walsh PS, Wilde JI, Tom EY, et al.** Analytical performance verification of a molecular diagnostic for cytology-indeterminate thyroid nodules. *J Clin Endocrinol Metab*. 2012;97:E2297–E2306.
5. **Sigstad E, Paus E, Bjoro T, et al.** The new molecular markers DDIT3, STT3A, ARG2 and FAM129A are not useful in diagnosing thyroid follicular tumors. *Mod Pathol*. 2012;25:537–547.
6. **Dibner C, Schibler U, Albrecht U.** The mammalian circadian timing system: organization and coordination of central and peripheral clocks. *Annu Rev Physiol*. 2010;72:517–549.
7. **Nagoshi E, Saini C, Bauer C, Laroche T, Naef F, Schibler U.** Circadian gene expression in individual fibroblasts: cell-autonomous and self-sustained oscillators pass time to daughter cells. *Cell*. 2004; 119:693–705.
8. **Kowalska E, Ripperger JA, Hoegger DC, et al.** NONO couples the circadian clock to the cell cycle. *Proc Natl Acad Sci USA*. 2013;110: 1592–1599.
9. **Matsuo T, Yamaguchi S, Mitsui S, Emi A, Shimoda F, Okamura H.** Control mechanism of the circadian clock for timing of cell division in vivo. *Science*. 2003;302:255–259.
10. **Fu L, Pelicano H, Liu J, Huang P, Lee C.** The circadian gene Period2 plays an important role in tumor suppression and DNA damage response in vivo. *Cell*. 2002;111:41–50.
11. **Sancar A, Lindsey-Boltz LA, Kang TH, Reardon JT, Lee JH, Ozturk N.** Circadian clock control of the cellular response to DNA damage. *FEBS Lett*. 2010;584(12):2618–2625.
12. **Hua H, Wang Y, Wan C, et al.** Circadian gene mPer2 overexpression induces cancer cell apoptosis. *Cancer Sci*. 2006;97:589–596.
13. **Levi F, Okyar A, Dulong S, Innominato PF, Clairambault J.** Circadian timing in cancer treatments. *Annu Rev Pharmacol Toxicol*. 2010;50:377–421.
14. **Haus E.** Chronobiology in the endocrine system. *Adv Drug Deliv Rev*. 2007;59:985–1014.
15. **DeLellis R, Lloyd R, Heitz P, Eng C, The International Agency for Research on Cancer.** In: Lloyd R, Heitz P, Eng C, eds. *Pathology and Genetics of Tumours of Endocrine Organs* (International Agency for Research on Cancer-World Health Organization Classification of Tumours). International Agency for Research on Cancer; 2004.
16. **Dibner C, Sage D, Unser M, Bauer C, et al.** Circadian gene expression is resilient to large fluctuations in overall transcription rates. *EMBO J*. 2009;28:123–134.
17. **Pulimeno P, Mannic T, Sage D, et al.** Autonomous and self-sustained circadian oscillators displayed in human islet cells. *Diabetologia*. 2013;56:497–507.
18. **Liu AC, Tran HG, Zhang EE, Priest AA, Welsh DK, Kay SA.** Redundant function of REV-ERBα and β and non-essential role for Bmal1 cycling in transcriptional regulation of intracellular circadian rhythms. *PLoS Genet*. 2008;4(2):e1000023.
19. **Marler MR, Gehrman P, Martin JL, Ancoli-Israel S.** The sigmoidally transformed cosine curve: a mathematical model for circadian rhythms with symmetric non-sinusoidal shapes. *Stat Med*. 2006;25: 3893–3904.
20. **Wasenius VM, Hemmer S, Kettunen E, Knuutila S, Franssila K, Joensuu H.** Hepatocyte growth factor receptor, matrix metalloproteinase-11, tissue inhibitor of metalloproteinase-1, and fibronectin are up-regulated in papillary thyroid carcinoma: a cDNA and tissue microarray study. *Clin Cancer Res*. 2003;9:68–75.
21. **Hawthorn L, Stein L, Varma R, Wiseman S, Loree T, Tan D.** TIMP1 and SERPIN-A overexpression and TFF3 and CRABP1 underexpression as biomarkers for papillary thyroid carcinoma. *Head Neck*. 2004;26:1069–1083.
22. **Balsalobre A, Brown SA, Marcacci L, et al.** Resetting of circadian time in peripheral tissues by glucocorticoid signaling. *Science*. 2000; 289:2344–2347.
23. **Brown SA, Fleury-Olela F, Nagoshi E, et al.** The period length of fibroblast circadian gene expression varies widely among human individuals. *PLoS Biol*. 2005;3:e338.
24. **Yoo SH, Yamazaki S, Lowrey PL, et al.** PERIOD2::LUCIFERASE real-time reporting of circadian dynamics reveals persistent circadian oscillations in mouse peripheral tissues. *Proc Natl Acad Sci USA*. 2004;101:5339–5346.
25. **Schmidt EE, Schibler U.** High accumulation of components of the RNA polymerase II transcription machinery in rodent spermatids. *Development*. 1995;121:2373–2383.
26. **Kalsbeek A, van der Spek R, Lei J, Endert E, Buijs RM, Fliers E.** Circadian rhythms in the hypothalamo-pituitary-adrenal (HPA) axis. *Mol Cell Endocrinol*. 2012;349:20–29.
27. **Sviridonova MA, Fadeyev VV, Sych YP, Melnichenko GA.** Clinical significance of TSH circadian variability in patients with hypothyroidism. *Endocr Res*. 2013;38:24–31.
28. **Jazdzewski K, Boguslawska J, Jendrzejewski J, et al.** Thyroid hormone receptor β (THRB) is a major target gene for microRNAs deregulated in papillary thyroid carcinoma (PTC). *J Clin Endocrinol Metab*. 2011;96:E546–E553.
29. **Hughes ME, Hogenesch JB, Kornacker K.** JTK_CYCLE: an efficient nonparametric algorithm for detecting rhythmic components in genome-scale data sets. *J Biol Rhythms*. 2010;25:372–380.
30. **Straume M.** DNA microarray time series analysis: automated statistical assessment of circadian rhythms in gene expression patterning. *Methods Enzymol*. 2004;383:149–166.
31. **Yang R, Su Z.** Analyzing circadian expression data by harmonic

The Endocrine Society. Downloaded from press.endocrine.org by [${individualUser.displayName}] on 04 May 2015. at 05:40 For personal use only. No other uses without permission. . All rights reserved.

regression based on autoregressive spectral estimation. *Bioinformatics*. 2010;26:i168–i174.
32. **Chen ST, Choo KB, Hou MF, Yeh KT, Kuo SJ, Chang JG.** Deregulated expression of the PER1, PER2 and PER3 genes in breast cancers. *Carcinogenesis*. 2005;26:1241–1246.
33. **Gaddameedhi S, Selby CP, Kaufmann WK, Smart RC, Sancar A.** Control of skin cancer by the circadian rhythm. *Proc Natl Acad Sci USA*. 2011;108:18790–18795.
34. **Hsu CM, Lin SF, Lu CT, Lin PM, Yang MY.** Altered expression of circadian clock genes in head and neck squamous cell carcinoma. *Tumour Biol*. 2012;33:149–155.
35. **Relles D, Sendecki J, Chipitsyna G, Hyslop T, Yeo CJ, Arafat HA.** Circadian gene expression and clinicopathologic correlates in pancreatic cancer. *J Gastrointest Surg*. 2013;17:443–450.
36. **Yang MY, Yang WC, Lin PM, et al.** Altered expression of circadian clock genes in human chronic myeloid leukemia. *J Biol Rhythms*. 2011;26:136–148.
37. **Kondratov RV, Kondratova AA, Gorbacheva VY, Vykhovanets OV, Antoch MP.** Early aging and age-related pathologies in mice deficient in BMAL1, the core component of the circadian clock. *Genes Dev*. 2006;20:1868–1873.

EndoGrants CentralTM features **funding opportunities of interest** to the endocrine community, saving you time and effort.

www.endocrine.org/grants

The Endocrine Society. Downloaded from press.endocrine.org by [${individualUser.displayName}] on 04 May 2015. at 05:40 For personal use only. No other uses without permission. . All rights reserved.